Gated Channel Transformation for Visual Recognition

Anonymous authors
Paper under double-blind review

Abstract

In this work, we propose a generally applicable transformation unit for visual recognition with deep convolutional neural networks. This transformation explicitly models channel relationships with explainable control variables. These variables determine the neuron behaviors of competition or cooperation, and they are jointly optimized with convolutional weights towards more accurate recognition. In Squeeze-and-Excitation (SE) Networks, the channel relationships are implicitly learned by fully connected layers, and the SE block is integrated at the block-level. We instead introduce a channel normalization layer to reduce the number of parameters and computational complexity. This lightweight layer incorporates a simple l_2 normalization, enabling our transformation unit applicable to operator-level without much increase of additional parameters. Extensive experiments demonstrate the effectiveness of our unit with clear margins on many vision tasks, i.e., image classification on ImageNet, object detection and instance segmentation on COCO, video classification on Kinetics.

1 Introduction

Convolutional Neural Networks (CNNs) have proven to be critical and robust in visual recognition tasks, such as image classification (Huang et al., 2018), detection (Singh et al., 2018), and segmentation (Singh et al., 2018). Notably, a single convolutional layer operates only on a neighboring local context of each spatial position of a feature map, which could possibly lead to local ambiguities (Torralba, 2003; Hu et al., 2018a). To relief this problem, VGGNets (Simonyan & Zisserman, 2015) were proposed to construct deep CNNs, using a series of convolutional layers with non-linear activation functions and downsampling operators to cover a large extent of context. Moreover, (He et al., 2016a;b) introduced a residual connection to help CNNs benefit from deeper architectures further.

Apart from improving the depth of CNNs, another branch of methods focuses on augmenting convolutional layer with modules that directly operate on context across large neighborhoods. Squeeze-and-Excitation Networks (SE-Net) (Hu et al., 2018b) leveraged globally embedding information to model channel relationship and modulate feature maps on the channel-wise level. Moreover, its following method, GE-Net (Hu et al., 2018a), used largely neighboring embedding instead. These modules can be conveniently assembled into modern networks, such as ResNet and Inception (Szegedy et al., 2015; 2016; 2017) networks, to improve the representational ability of networks.

However, the SE module uses two fully connected (*FC*) layers to process channel-wise embeddings, which leads to two problems. First, the number of SE modules to be applied in CNNs is limited. In Hu et al. (2018b), SE module was applied at the block-level, i.e., a single SE module is utilized per Res-block (He et al., 2016a) or Inception-block (Szegedy et al., 2016). The dimension of the *FC* layer is decreased to save the computational cost further. However, the designed *FC* layers still hinder the wide deployment of SE modules across all layers. Second, due to the complexity of the parameters in *FC* (or convolutional layer in GE-Net), it is difficult to analyze the interactions among the channels at different layers. The channel relationships learned by convolution and FC operations are inherently implicit (Hu et al., 2018b), resulting in agnostic behaviors of the neuron outputs.

In this paper, we propose a Gated Channel Transformation (GCT) for efficient and accurate contextual information modeling. First, we use a normalization component to replace the *FC* layers. Normalization methods, e.g., Local Response Normalization (LRN) (Krizhevsky et al., 2012), create competitions among different neurons in neural networks. Batch normalization (Ioffe & Szegedy, 2015) and its variants can smooth gradient and have been widely used in accelerating CNNs training process (Ioffe & Szegedy, 2015; Wu & He, 2018). We leverage a simple l_2 normalization for modeling channel relationship, which is more stable and computationally efficient comparing to FC layers. Second, we introduce a few channel-wise parameters to control the behavior of the gated adaptation of feature channels. Compared to the large number of parameters in FC, our designed parameters are much more lightweight. Besides, the gating weight parameter is convenient for channel relationship analysis and is helpful to understand the effect of GCT modules across different layers. According to our visualization analysis, GCT prefers to encourage cooperation in shallower layers, but competition is enhanced in deeper layers.

Our experiments show that GCT is a simple and effective architecture for modeling relationship among channels. It significantly improves the generalization capability of deep convolutional networks across visual recognition tasks and datasets.

2 Related Work

Gating and attention mechanisms. Gating mechanisms have been successfully deployed in some recurrent neural network architectures. Long Short-Term Memory (LSTM) (Hochreiter & Schmidhuber, 1997) introduced an input gate, output gate and forget gate, which are used to regulate the flow of information into and out of the module. Based on gating mechanisms, some attention methods focus on forcing computational resources towards the most informative components of features (Larochelle & Hinton, 2010; Mnih et al., 2014; Vaswani et al., 2017). Recent works introduce the attention mechanism into convolutional networks (Gehring et al., 2017; Dauphin et al., 2017; Woo et al., 2018; Park et al., 2018). Following these studies, SE-Nets (Hu et al., 2018b) and its following work GE-Nets (Hu et al., 2018a) introduced a lightweight gating mechanism which focuses on enhancing the representational power of the convolutional network by modeling channel-wise relationship. Compared to the SE module, our GCT also pays attention to the cross-channel relationship but can achieve better performance gains with less computation and parameters.

Normalization layers. In recent years, normalization layers have been widely used in deep networks to create competition between neurons (Krizhevsky et al., 2012) and produce smoother optimization surfaces (Ioffe & Szegedy, 2015). Local Response Normalization (LRN) (Lyu & Simoncelli, 2008; Jarrett et al., 2009; Krizhevsky et al., 2012) computes the statistics in a small neighborhood among channels for each pixel. Batch Normalization (BN) (Ioffe & Szegedy, 2015) utilizes global spatial information along the batch dimension and suggests to be deployed for all layers. Layer Normalization (LN) (Ba et al., 2016) computes along the channel dimension instead of the batch dimension. Group Normalization (GN) (Wu & He, 2018) differently divides the channels into groups and computes within each group the mean and variance for normalization. Similar to LRN, GN and LN, our GCT also utilizes channel-related information with normalization structure.

Deep architectures. VGGNets (Simonyan & Zisserman, 2015) and Inception networks (Szegedy et al., 2015) demonstrated that it was significant to improve the quality of representation by increasing the depth of a network. ResNets (He et al., 2016a) utilized shortcut connections to identity-based skip connections, and proved that it was highly effective to build considerably deeper and stronger networks with them. Some other researchers focused on improving the representation ability of the computational elements contained within a network (Szegedy et al., 2016). The more diverse composition of operators within a computational element can be constructed with multi-branch convolutions or pooling layers. Other than this, grouped convolutions have proven to be a practical method to increase the cardinality of learned transformations (Xie et al., 2017). We build our GCT on these deep architectures. All these networks with GCT achieve promising performance improvements, but the growth of computational complexity is negligible.

3 Gated Channel Transformation

SE-Nets (Hu et al., 2018b) proposed a lightweight SE module to augment convolutional networks by operating on a global context. The SE module contains two operators, i.e., a "squeeze" operator to embed channel context and an "excitation" operator to modulate the feature maps. The architecture of our Gated Channel Transformation benefits from this framework. Differently, GCT

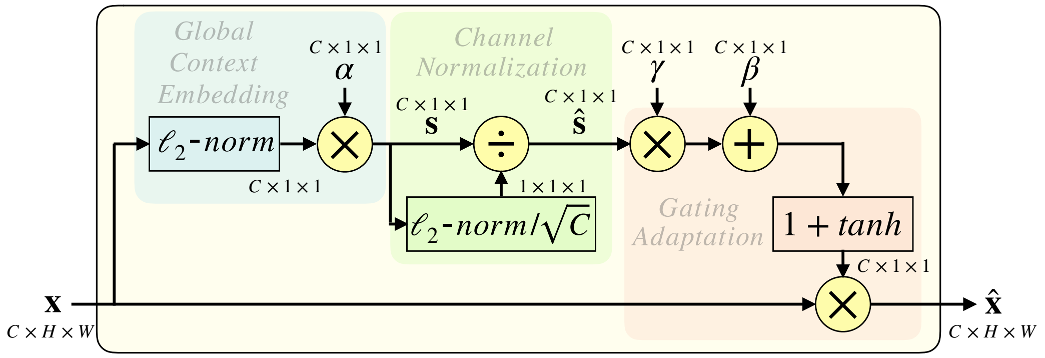

Figure 1: An **overview** of the structure of Gated Channel Transformation (GCT).

leverages a normalization operator instead of the *FC* layers in the SE module for channel relationship modeling. Notably, the normalization operator is parameter-free. To make GCT learnable, we redesign the structure of the "squeeze" and "excitation" operators. Our new operators contain three sets of channel-wise trainable parameters. Thus, GCT is more convenient to be deployed occupying a small number of parameters. The gating parameters can be visualized for easier analysis of GCT's behavior, while the discriminative ability is maintained.

Let $\mathbf{x} \in \mathbb{R}^{C\times H\times W}$ be an activation feature in a convolutional network, where H and W are the spatial height and width, and C is the number of channels. In general, GCT performs the following transformation:

$$\hat{\mathbf{x}} = F(\mathbf{x}|\boldsymbol{\alpha}, \boldsymbol{\gamma}, \boldsymbol{\beta}), \boldsymbol{\alpha}, \boldsymbol{\gamma}, \boldsymbol{\beta} \in \mathbb{R}^{C}. \tag{1}$$

Here $\boldsymbol{\alpha}$, $\boldsymbol{\gamma}$ and $\boldsymbol{\beta}$ are trainable parameters. Embedding weights $\boldsymbol{\alpha}$ are responsible for adapting the embedding outputs. The gating weights $\boldsymbol{\gamma}$ and biases $\boldsymbol{\beta}$ control the activation of the gate. They determine the behavior of GCT in each channel. The parameter complexity of GCT is $O(C)$, which is smaller than the SE module ($O(C^2)$) (Hu et al., 2018b). In SE-Net, two *FC* layers are leveraged, which have the parameter complexity of $O(C^2)$.

An illustration of the structure of GCT is shown in Fig. 1. Let $\mathbf{x} = [x_1, x_2, ..., x_C], x_c = [x_c^{i,j}]_{H\times W} \in \mathbb{R}^{H\times W}, c \in \{1, 2, ..., C\}$, where x_c is corresponding to each channel of $\mathbf{x}$. The detailed transformation consists of following parts.

Global Context Embedding. Global context embedding (GCE) aggregates global context in each channel. GCE can exploit global contextual information outside the small receptive fields of convolutional layers. Given the embedding weights $\boldsymbol{\alpha} = [\alpha_1, ..., \alpha_C]$, GCE is defined as:

$$s_c = \alpha_c ||x_c||_2 = \alpha_c\{[\sum_{i=1}^{H}\sum_{j=1}^{W}(x_c^{i,j})^2] + \epsilon\}^{\frac{1}{2}}, \tag{2}$$

where ϵ is a small constant to avoid the problem of derivation at the zero point. Different from SE, GCT does not use global average pooling (GAP) to aggregate channel context. GAP might fail in some extreme cases. For example, if SE is deployed after the Instance Normalization (IN) (Ulyanov et al., 2016) layer that is popular in style transfer task, the output of GAP will be constant for any inputs since IN fixes the mean of each channel of features. To avoid this problem, we choose ℓ_p-norm instead. It is worth noting that GCT is robust with different ℓ_p-norms. In Sec. 4.5, we compare the performance of some popular ℓ_p-norms and choose the best one, ℓ_2-norm, to be our default setting. Notably, the performance of ℓ_1-norm is very close to ℓ_2-norm and ℓ_1-norm can be equivalently replaced by GAP when the input of GCT is always non-negative (for example, after ReLU activation). In this case, ℓ_1-norm is more computationally efficient.

Besides, we use trainable parameters α_c to adjust each channel because different channels should have different significance.

Channel Normalization. Normalization methods can model relationship in visual or photographic features (Lyu & Simoncelli, 2008) with lightweight computing resource (*e.g.*, Ioffe & Szegedy (2015)). Similar to Local Response Normalization (LRN) (Krizhevsky et al., 2012), we use a ℓ_2 normalization to operate across channels, namely channel normalization (CN). Let $\mathbf{s} = [s_1, ..., s_C]$, the formula of CN is:

$$\hat{s}_c = \frac{\sqrt{C}s_c}{||\mathbf{s}||_2} = \frac{\sqrt{C}s_c}{[(\sum\limits_{c=1}^{C} s_c^2) + \epsilon]^{\frac{1}{2}}}, \tag{3}$$

where ϵ is a small constant. The scalar $\sqrt{C}$ is used to normalize the scale of $\hat{s}_c$, avoiding a too small scale of $\hat{s}_c$ when C is large. Compared to the *FC* layers used by SE (Hu et al., 2018b), our CN operator has less computational complexity ($O(C)$) compared to the *FC* layers ($O(C^2)$).

Gating Adaptation. We employ a gating mechanism, namely gating adaptation (GA), to adapt the original feature. By introducing the gating mechanism, our GCT can facilitate both competition and cooperation during the training process. Let the gating weights $\boldsymbol{\gamma} = [\gamma_1, ..., \gamma_C]$ and the gating biases $\boldsymbol{\beta} = [\beta_1, ..., \beta_C]$, we design the following gating function:

$$\hat{x}_c = x_c[1 + \tanh(\gamma_c \hat{s}_c + \beta_c)]. \tag{4}$$

The scale of each original channel x_c will be adapted by its corresponding gate, i.e., $1 + \tanh(\gamma_c \hat{s}_c + \beta_c)$. The trainable γ_c and β_c are employed to control the activation of gate. LRN benefits from only the competitions among the neurons (Krizhevsky et al., 2012). However, the gating mechanism in GCT is able to create both competition and cooperation among different channels. This capability is more consistent with the training process in biological neural networks (Demin & Nekhaev, 2018). When the gating weight of one channel (γ_c) is activated positively, GCT promotes this channel to compete with the others as in LRN. When the gating weight is activated negatively, GCT encourages this channel to cooperate with the others. We analyze these adaptive channel relationships in Sec.4.4.

Besides, this gate function allows original features to pass to the next layer when the gating weights and biases are zeros, which is

$$\hat{\mathbf{x}} = F(\mathbf{x}|\boldsymbol{\alpha}, \mathbf{0}, \mathbf{0}) = \mathbf{1}\mathbf{x} = \mathbf{x}. \tag{5}$$

The ability of modeling identity mapping can effectively improve the robustness to the degradation problem in deep networks. ResNet (He et al., 2016a) also benefits from this idea. Therefore, we propose to initialize $\boldsymbol{\gamma}$ and $\boldsymbol{\beta}$ to 0 in the initialization of GCT layers. By doing this, the initial steps of the training process will be more stable, and the final performance of GCT will be better.

4 EXPERIMENTS

We apply GCT for all the convolutional layers in deep networks rather than block-level deployment in SE-Net. In all GCT counterparts, we employ one GCT layer before each convolutional layer. In the Kinetics experiments, we apply GCT at the last two convolutional layers in each Res-Block. More training details are shown in Appendix A.

4.1 EXPERIMENTS ON IMAGENET

We experiment on the ImageNet 2012 dataset (Russakovsky et al., 2015) with $1,000$ classes. We train all the models on the 1.28M training images and evaluate on the $50,000$ validation images. We also conduct classification experiments on CIFAR (Krizhevsky & Hinton, 2009) in Appendix B.

Implementation details. In the training process of all the models, the input image is 224×224 randomly cropped from a resized image using the same augmentation in Szegedy et al. (2015). We use SGD with a mini-batch size of 256. For ResNet-152 and ResNeXt-50, we use half mini-batch size and double the training steps). The weight decay is 0.0001, and the momentum is 0.9. The base learning rate is 0.1, and we divide it by 10 every 30 epochs. All models are trained for 100 epochs from scratch, using the weight initialization strategy described in He et al. (2015). Besides, we start the training process with a learning rate of 0.01 for 1 epoch. After the warmup, we go back to the original learning rate schedule. In all comparisons, we evaluate the error on the single 224×224 center crop from an image whose shorter side is 256. For ResNet-200 (He et al., 2016b), we evaluate on 320×320 following He et al. (2016b).

Integration with deep modern architectures. We study the effects of integrating GCT layers with some state-of-the-art backbone architectures, e.g., ResNet (He et al., 2016a) and ResNeXt (Xie et al., 2017), in which we apply GCT before all the convolutional layers. We report all these results in Table 1. Compared to original architectures, we observe significant performance improvements

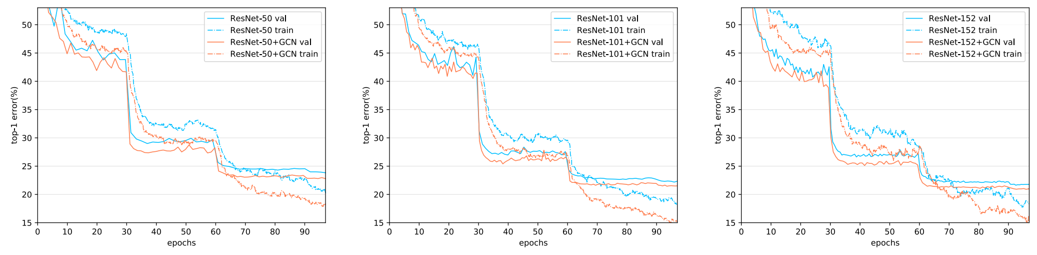

(a) ResNet-50 (b) ResNet-101 (c) ResNet-152

Figure 2: **Training curve comparisons** for ResNets with different depth on ImageNet.

Table 1: **Improvement in error performance (%) on ImageNet.** The numbers in brackets denote the improvement in performance over the baselines. ResNet-200* means we follow the strategy in He et al. (2016b) to train this model on 224×224 but evaluate on 320×320.

	original		**GCT**	
Network	top-1	top-5	top-1	top-5
VGG-16 (Simonyan & Zisserman, 2015)	26.2	8.3	**25.1**$_{(1.1)}$	**7.5**$_{(0.8)}$
Inception-v3 (Szegedy et al., 2016)	24.3	7.3	**23.7**$_{(0.6)}$	**7.1**$_{(0.2)}$
ResNeXt-50 (Xie et al., 2017)	22.4	6.3	**21.7**$_{(0.7)}$	**6.0**$_{(0.3)}$
ResNet-50 (He et al., 2016a)	23.8	7.0	**22.7**$_{(1.1)}$	**6.3**$_{(0.7)}$
ResNet-101 (He et al., 2016a)	22.2	6.2	**21.4**$_{(0.8)}$	**5.9**$_{(0.3)}$
ResNet-152 (He et al., 2016a)	21.6	5.9	**20.8**$_{(0.8)}$	**5.5**$_{(0.4)}$
ResNet-200* (He et al., 2016b)	20.7	5.2	**19.7**$_{(1.0)}$	**4.8**$_{(0.4)}$

by introducing GCT into networks. Particularly, the top-1 error of GCT-ResNet-101 is $\mathbf{21.4}\%$, which is even better than the ResNet-152 baseline (21.6%) with a deeper network and much more parameters. In addition, GCT is able to bring stable improvement in ResNets with different depth ($\mathbf{1.1}\%$ top-1 improvement in ResNet-50, $\mathbf{0.8}\%$ in ResNet-152 and $\mathbf{1.0}\%$ in ResNet-200). Besides, we observe a smooth improvement throughout the training schedule, which is shown in Fig.2.

We also explore the improvement with GCT in *non-residual* networks (*e.g.*, VGG-16 (Simonyan & Zisserman, 2015) and Inception-v3 (Szegedy et al., 2016)). To stabilize the training process, we employ BN (Ioffe & Szegedy, 2015) layers after every convolutional layer. Similar to the effectiveness in residual architectures, GCT layers bring promising improvements in *non-residual* structures.

Compared to SE. We conduct experiments on ImageNet to compare SE with GCT in both residual and *non-residual* networks and the results are reported in Table 2. We follow the methods in Hu et al. (2018b) to integrate SE into VGG-16 (Simonyan & Zisserman, 2015), Inception (Szegedy et al., 2016), ResNet-50 (He et al., 2016a) and ResNeXt-50 (Xie et al., 2017) and train these models in same training schedule. Compared to SE, GCT always achieves better improvement.

In order to compare computational complexity, we calculate the GFLOPs and the number of parameters. In VGG-16 experiments, SE is employed for all the convolutional layers, which is the same as GCT. Under this fair condition, GCT achieves better performance with less increase in both GFLOPs (**0.019**G *vs*.0.028G) and parameters (**0.01**M *vs*.0.23M). In other experiments, SE is only employed in block-level (Res-Block or Inception-Block) as proposed (Hu et al., 2018b), which means the number of SE is smaller than GCT. However, the increase in parameters of GCT is still much less than SE, and the value of GFLOPs is comparable. Compared to SE, the increase in parameters of GCT is negligible, but the performance is better.

4.2 Experiments on COCO

Next we evaluate the generalizability on the COCO dataset (Lin et al., 2014). We train the models on the COCO *train2017* set and evaluate on the COCO *eval2017* set (a.k.a *minival*).

Implementation details. We experiment on the Mask R-CNN baselines (He et al., 2017) and its GN counterparts (Wu & He, 2018). All the backbone models are pre-trained on ImageNet using the scale and aspect ratio augmentation in Szegedy et al. (2015) and fine-tune on COCO with a batch size of 16 (2 images/GPU). Besides, all these experiments use the Feature Pyramid Network

Table 2: **Compared to SE in different networks on ImageNet.** We evaluate the models of error performance (%), GFLOPs (G) and parameters (M). G/P means GFLOPs/parameters. In VGG-16 experiments, SE is employed for all the convolutional layers, which is the same as GCT. In other experiments, SE is only employed in block level (Res-Block or Inception-Block) as proposed (Hu et al., 2018b). This difference makes that SE uses comparable GFLOPs with GCT.

	original		SE		**GCT (ours)**	
Network	top-1/5	G/P	top-1/5	G/P	top-1/5	G/P
ResNet-50	23.8/7.0	3.879/25.61	22.9/6.6	**3.893**/28.14	**22.7/6.3**	3.900/**25.68**
ResNeXt-50	22.4/6.3	3.795/25.10	22.0/6.1	**3.809**/27.63	**21.7/6.0**	3.821/**25.19**
VGG-16	26.2/8.3	15.497/138.37	25.2/7.7	15.525/138.60	**25.1/7.5**	**15.516/138.38**
Inception-v3	24.3/7.3	2.847/23.87	24.0/7.2	**2.851**/25.53	**23.7/7.1**	2.862/**23.99**

Table 3: **Improvement on COCO with Mask R-CNN framework.** The numbers in brackets denote the improvement in performance over the baselines. BN* means BN is frozen. $^+$ means increasing the training iterations from 90K to 270K. When using GN, we follow the strategy in the original paper (Wu & He, 2018).

Backbone	box head	box AP	mask AP
ResNet-50 BN*	-	37.8	34.2
ResNet-50 BN*+**GCT**	-	**39.8**$_{(2.0)}$	**36.0**$_{(1.8)}$
ResNet-101 BN*	-	40.1	36.1
ResNet-101 BN*+**GCT**	-	**42.0**$_{(1.9)}$	**37.7**$_{(1.6)}$
$^+$ResNet-50 BN*	-	38.6	34.5
$^+$ResNet-50 GN	GN	40.8$_{(2.2)}$	36.1$_{(1.6)}$
$^+$ResNet-50 BN*+**GCT**	GN	**41.6**$_{(3.0)}$	**37.1**$_{(2.6)}$
$^+$ResNet-50 BN*+**GCT**	GN+**GCT**	**41.8**$_{(3.2)}$	**37.3**$_{(2.8)}$
$^+$ResNet-101 BN*	-	40.9	36.4
$^+$ResNet-101 GN	GN	42.3$_{(1.4)}$	37.2$_{(0.8)}$
$^+$ResNet-101 BN*+**GCT**	GN	**43.1**$_{(2.2)}$	**38.3**$_{(1.9)}$

(FPN) (Lin et al., 2017). We also use the same hyperparameters and two training schedules used in Wu & He (2018). The short schedule includes 90K iterations, in which the learning rate is divided by 10 at 60K and 80K iterations. The long schedule increases the iterations to 270K, in which the learning rate is divided by 10 at 210K and 250K. The base learning rate is 0.02 in both schedules.

Improvements on Mask R-CNN. Table 3 shows the comparison of BN* (frozen BN), GN and BN*+GCT (using GCT before all the convolutional layers of the backbones). First, we use a short training schedule to compare baselines and GCT counterparts. GCT shows stable and significant improvement in both ResNet-50 and ResNet-101. In ResNet-50, GCT improves detection AP by $\mathbf{2.0}$ and segmentation AP by $\mathbf{1.8}$. Moreover, in ResNet-101, GCT also improves detection AP by $\mathbf{1.9}$ and segmentation AP by $\mathbf{1.6}$. Then, we use the long schedule to compare GN and BN*+GCT. GN is more effective than BN when batch size is small as in this case of detection and segmentation using Mask R-CNN. However, we deploy GCT together with BN into the backbone, and these BN*+GCT counterparts achieve much better performance than GN backbones. Compared to GN in ResNet-101, BN*+GCT improves detection AP by $\mathbf{0.8}$ and segmentation AP by $\mathbf{1.1}$. In particular, ResNet-101 with BN*+GCT trained in the short schedule achieves better segmentation AP ($\mathbf{37.7}$) than the GN counterpart (37.2) trained with the long schedule. This GN counterpart also uses GN in the backbone, the box heads, and the FPN. We also explore to combine GCT with GN by introducing GCT into GN box head. The results show GN+GCT achieves a better performance. It demonstrates the benefits of integrating GCT with GN. We now have shown the effectiveness of GCT in working with both BN and GN.

4.3 Experiments on Kinetics

Our previous experiments demonstrate the effectiveness of GCT on image-related tasks. We now evaluate the generalizability in video understanding task of action recognition on the large scale Kinetics-400 (Kay et al., 2017) dataset. We employ the ResNet-50 (3D) and ResNet-101 (3D) as the backbone and apply GCT in the last two convolutional layers in each Res-Block. The backbone networks are pre-trained on ImageNet (Russakovsky et al., 2015).

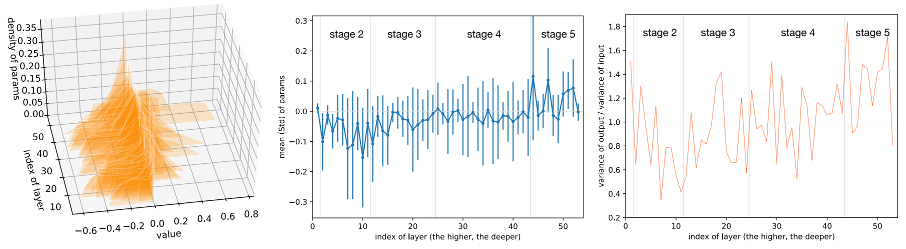

(a) distribution of γ (b) mean (std) of γ (c) ratio of the variance of output and input

Figure 3: **Analysis**. The visulization of parameters of γ (Fig.(a), (b)), and the ratio of variance of GCT output and input feature (Fig.(c)) in all the GCT layers in ResNet-50 on ImageNet.

We compare with the state-of-the-art Non-Local Networks (NL-Net) (Wang et al., 2018). The results show that GCT counterparts consistently improves the recognition accuracy over both the ResNet-50 and ResNet-101 baselines, as shown in Table 4. Because of our limited memory resource, we can **NOT** apply GCT in all the convolutional layers, which we believe can further improve the performance.

In summary, extensive experiments demonstrate that GCT is effective across a wide range of architectures, tasks, and datasets.

4.4 Analysis

To analyze the behavior of GCT in different layers, we visualize the distribution of the gating weights (γ) of each GCT layer in ResNet-50 on ImageNet. Further, we sort these distributions according to their layer index in 3D space (Fig. 3a). The bigger layer index means it is closer to the network output. To make the visualization clearer, we re-scale the vertical z axis with $log(1+z)$, which corresponds to the percentage density of γ. We also calculate the mean and standard deviation (std) of γ in each layer and show them in a bar chart (Fig. 3b). As shown in Fig. 3a and 3b, the mean of γ tends to be less than 0 in the GCT layers far from the network output. Oppositely, in the layers close to the output, the mean tends to be greater than 0.

According to Eq. 3 & 4, the adaptation of channel x_c is related to $\hat{s}_c$, which corresponds to the ratio of the weighted ℓ_2-norm of x_c (i.e., s_c) and the average of all the s_c. When the gating weight γ_c is greater than 0, the adaptation is positively correlated to $\hat{s}_c$ and increases the variance between x_c and others; When γ_c is lower than 0, the adaptation is negatively correlated and reduces the variance.

Based on the analysis and the results we observe, we suppose that GCT tends to reduce the difference among channels in layers far away from the output. This behavior is helpful to encourage cooperation among channels and relieve overfitting. Apart from this, GCT tends to increase the difference among channels when close to the output. Here, GCT acts like the attention mechanism that is useful for creating competition.

To further validate our hypothesis, we calculate the ratio of the variance of output and input feature of each GCT layer, which we show in Fig. 3c. More visualizations are shown in Appendix C. Generally, the shallow layers learn low-level features to capture general characteristics like textures, edges, and corners. The feature variances become larger in deeper layers, where the high-level features are more discriminative and task-related. As expected, in the layers close to network output, GCT tends to magnify the variance of input feature (the ratio is always greater than 1), but in the layers far away from the output, GCT tends to reduce the variance (the ratio is always less than 1). This phenomenon is consistent with our previous hypothesis and shows that GCT is effective in creating both competition and cooperation among channels. Our observation validates that GCT can adaptively learn the channel relationships at different layers.

4.5 Ablation Studies.

In this section, we conduct a serial of ablation experiments to explain the relative importance of each operator in the GCT. At last, we show how the performance changes with regards to the GCT position in a network.

Table 4: **Improvement in top-1 accuracy (%) over the state-of-the-art method on Kinetics.** The numbers in brackets denote the improvement in performance over the baselines.

Backbone	NL-Net	**GCT**
ResNet-50	74.6	$\mathbf{75.1}_{(0.5)}$
ResNet-101	75.7	$\mathbf{76.2}_{(0.5)}$

Table 5: **Ablation experiments.** We evaluate error performance in GCT-ResNet-50 on ImageNet (%). The ResNet-50 baseline achieves a top-1 of 23.8 and a top-5 of 7.0.

(a) Embedding operator.

Norm	top-1	top-5
ℓ_∞	23.1	6.7
ℓ_1	22.8	6.3
ℓ_2	**22.7**	**6.3**

(b) Normalization operator.

Normalization	top-1	top-5
mean+variance	23.7	7.1
ℓ_1	22.9	6.4
ℓ_2	**22.7**	**6.3**

(c) Adaptation operator.

Adaptation	top-1	top-5
$Sigmoid$	22.9	6.5
$1 + ELU$	22.7	6.4
$1 + tanh$	**22.7**	**6.3**

(d) Application position.

Position	top-1	top-5
after BN	23.1	6.6
before BN	23.1	6.5
before Conv	**22.7**	**6.3**

Table 6: **Clock time comparison**. We calculate average inference times (ms) per batch by using 1 GTX 1080Ti with 16 batch size for 1,000 iterations on ImageNet. For the sake of fairness, the modules are applied for all the Convs in VGG-16.

	baseline	+SE	+GCT(ℓ_1-norm)	+GCT(ℓ_2-norm)
time(ms)/batch	51.11	$87.31_{36.20\uparrow}$	$\mathbf{59.46}_{\mathbf{8.35}\uparrow}$	$59.73_{8.62\uparrow}$

Embedding component. To explain the importance of ℓ_p-norm in GCE, we compare embedding operators with different ℓ_p norm. We report the results in Table 5a, which shows all the ℓ_p-norms are effective in GCE, but the ℓ_2-norm is slightly better than ℓ_1-norm. The results demonstrate the GCE of GCT is robust to different ℓ_p-norms. In addition, we make a clock time comparison between SE and GCTs with different embedding component. As shown in Table 6, ℓ_2-norm is computationally similar to ℓ_1-norm and GCT is much more efficient than SE ($\mathbf{8.62}ms \uparrow$ vs. $36.20ms \uparrow$).

Normalization component. We also explore the significance of ℓ_p-norm in CN by comparing ℓ_p normalization with mean and variance normalization. The mean and variance normalization will normalize mean to 0 and variance to 1, which is widely used in normalization layers (e.g., (Ioffe & Szegedy, 2015; Ba et al., 2016)). We show all these results in Table 5b. Particularly, mean and variance normalization achieves a top-1 error of 23.7%, which is only slightly better than the ResNet-50 baseline (23.8%). Both ℓ_1 and ℓ_2 normalization make more promising improvements, and ℓ_2 performs slightly better. ℓ_p normalization is better at representation learning in channel normalization.

Adaptation component. We replace the activation function of GA with a few different non-linear activation functions and show the results in Table 5c. Compare to the baseline (top-1 of 23.8%), all the non-linear adaptation operator achieves promising performance, and $1+tanh$ achieves a slightly better improvement. Both $1 + tanh$ and 1+ELU (Clevert et al., 2015) can model identity mapping, and achieve better results than $Sigmoid$. These strong results show that GCT is also robust to the choice of activation functions and the identity mapping is important in training.

Application position. To find the best way to deploy GCT layers, we conduct experiments in ResNet-50 architecture on ImageNet by separately applying GCT after all the BN layers, before all the BN layers, and before all the convolutional layers. The results are reported in Table 5d. All the placement methods are effective in using GCT to improve the representational power of networks. However, it is better to employ GCT before all the convolutional layers, which is similar to the strategy in Krizhevsky et al. (2012) (normalization after ReLU).

5 Conclusion and Future Work

In this paper, we propose GCT, a novel layer that effectively improves the discriminability of deep CNNs by leveraging the relationship among channels. Benefit from the design of combining normalization and gating mechanisms, GCT can facilitate two types of neuron relations, i.e., competition and cooperation, with negligible complexity of parameters. We conduct expensive experiments to show the effectiveness and robustness of GCT across a wide range of modern CNNs and datasets. In future work, we will study the feasibility to apply GCT into recurrent networks.

REFERENCES

Jimmy Lei Ba, Jamie Ryan Kiros, and Geoffrey E Hinton. Layer normalization. *arXiv preprint arXiv:1607.06450*, 2016.

Djork-Arné Clevert, Thomas Unterthiner, and Sepp Hochreiter. Fast and accurate deep network learning by exponential linear units (elus). *arXiv preprint arXiv:1511.07289*, 2015.

Yann N Dauphin, Angela Fan, Michael Auli, and David Grangier. Language modeling with gated convolutional networks. In *ICML*, 2017.

Vyacheslav Demin and Dmitry Nekhaev. Recurrent spiking neural network learning based on a competitive maximization of neuronal activity. *Frontiers in neuroinformatics*, 12, 2018.

Jonas Gehring, Michael Auli, David Grangier, Denis Yarats, and Yann N Dauphin. Convolutional sequence to sequence learning. In *ICML*, 2017.

Kaiming He, Xiangyu Zhang, Shaoqing Ren, and Jian Sun. Delving deep into rectifiers: Surpassing human-level performance on imagenet classification. In *ICCV*, 2015.

Kaiming He, Xiangyu Zhang, Shaoqing Ren, and Jian Sun. Deep residual learning for image recognition. In *CVPR*, 2016a.

Kaiming He, Xiangyu Zhang, Shaoqing Ren, and Jian Sun. Identity mappings in deep residual networks. In *European conference on computer vision*, pp. 630–645. Springer, 2016b.

Kaiming He, Georgia Gkioxari, Piotr Dollár, and Ross Girshick. Mask r-cnn. In *ICCV*, 2017.

Sepp Hochreiter and Jürgen Schmidhuber. Long short-term memory. *Neural computation*, 9(8): 1735–1780, 1997.

Jie Hu, Li Shen, Samuel Albanie, Gang Sun, and Andrea Vedaldi. Gather-excite: Exploiting feature context in convolutional neural networks. In *Advances in Neural Information Processing Systems*, pp. 9401–9411, 2018a.

Jie Hu, Li Shen, and Gang Sun. Squeeze-and-excitation networks. In *CVPR*, 2018b.

Yanping Huang, Yonglong Cheng, Dehao Chen, HyoukJoong Lee, Jiquan Ngiam, Quoc V Le, and Zhifeng Chen. Gpipe: Efficient training of giant neural networks using pipeline parallelism. *arXiv preprint arXiv:1811.06965*, 2018.

Sergey Ioffe and Christian Szegedy. Batch normalization: Accelerating deep network training by reducing internal covariate shift. In *ICML*, 2015.

Kevin Jarrett, Koray Kavukcuoglu, Yann LeCun, et al. What is the best multi-stage architecture for object recognition? In *ICCV*, 2009.

Will Kay, Joao Carreira, Karen Simonyan, Brian Zhang, Chloe Hillier, Sudheendra Vijayanarasimhan, Fabio Viola, Tim Green, Trevor Back, Paul Natsev, et al. The kinetics human action video dataset. *arXiv preprint arXiv:1705.06950*, 2017.

Alex Krizhevsky and Geoffrey Hinton. Learning multiple layers of features from tiny images. Technical report, Citeseer, 2009.

Alex Krizhevsky, Ilya Sutskever, and Geoffrey E Hinton. Imagenet classification with deep convolutional neural networks. In *NIPS*, 2012.

Hugo Larochelle and Geoffrey E Hinton. Learning to combine foveal glimpses with a third-order boltzmann machine. In *NIPS*, 2010.

Tsung-Yi Lin, Michael Maire, Serge Belongie, James Hays, Pietro Perona, Deva Ramanan, Piotr Dollár, and C Lawrence Zitnick. Microsoft coco: Common objects in context. In *ECCV*. Springer, 2014.

Tsung-Yi Lin, Piotr Dollár, Ross Girshick, Kaiming He, Bharath Hariharan, and Serge Belongie. Feature pyramid networks for object detection. In *CVPR*, 2017.

Ilya Loshchilov and Frank Hutter. Sgdr: Stochastic gradient descent with warm restarts. *arXiv preprint arXiv:1608.03983*, 2016.

Siwei Lyu and Eero P Simoncelli. Nonlinear image representation using divisive normalization. In *CVPR*, 2008.

Volodymyr Mnih, Nicolas Heess, Alex Graves, et al. Recurrent models of visual attention. In *NIPS*, 2014.

Vinod Nair and Geoffrey E Hinton. Rectified linear units improve restricted boltzmann machines. In *ICML*, 2010.

Jongchan Park, Sanghyun Woo, Joon-Young Lee, and In So Kweon. Bam: bottleneck attention module. *arXiv preprint arXiv:1807.06514*, 2018.

Olga Russakovsky, Jia Deng, Hao Su, Jonathan Krause, Sanjeev Satheesh, Sean Ma, Zhiheng Huang, Andrej Karpathy, Aditya Khosla, Michael Bernstein, et al. Imagenet large scale visual recognition challenge. *IJCV*, 115(3):211–252, 2015.

Karen Simonyan and Andrew Zisserman. Very deep convolutional networks for large-scale image recognition. In *ICLR*, 2015.

Bharat Singh, Mahyar Najibi, and Larry S Davis. Sniper: Efficient multi-scale training. In *Advances in Neural Information Processing Systems*, pp. 9333–9343, 2018.

Christian Szegedy, Wei Liu, Yangqing Jia, Pierre Sermanet, Scott Reed, Dragomir Anguelov, Dumitru Erhan, Vincent Vanhoucke, and Andrew Rabinovich. Going deeper with convolutions. In *ICCV*, 2015.

Christian Szegedy, Vincent Vanhoucke, Sergey Ioffe, Jon Shlens, and Zbigniew Wojna. Rethinking the inception architecture for computer vision. In *CVPR*, 2016.

Christian Szegedy, Sergey Ioffe, Vincent Vanhoucke, and Alexander A Alemi. Inception-v4, inception-resnet and the impact of residual connections on learning. In *ICLR Workshop*, 2017.

Antonio Torralba. Contextual priming for object detection. *International journal of computer vision*, 53(2):169–191, 2003.

Dmitry Ulyanov, Andrea Vedaldi, and Victor Lempitsky. Instance normalization: The missing ingredient for fast stylization. *arXiv preprint arXiv:1607.08022*, 2016.

Ashish Vaswani, Noam Shazeer, Niki Parmar, Jakob Uszkoreit, Llion Jones, Aidan N Gomez, Łukasz Kaiser, and Illia Polosukhin. Attention is all you need. In *NIPS*, 2017.

Xiaolong Wang, Ross Girshick, Abhinav Gupta, and Kaiming He. Non-local neural networks. In *CVPR*, 2018.

Sanghyun Woo, Jongchan Park, Joon-Young Lee, and In So Kweon. Cbam: Convolutional block attention module. In *ECCV*, 2018.

Yuxin Wu and Kaiming He. Group normalization. In *ECCV*, 2018.

Saining Xie, Ross Girshick, Piotr Dollár, Zhuowen Tu, and Kaiming He. Aggregated residual transformations for deep neural networks. In *CVPR*, 2017.

A Training details

Same to modern normalization layers (e.g., BN (Ioffe & Szegedy, 2015)), we propose to apply GCT for all convolutional layers in deep networks. However, there are many different points nearby one convolutional layer to employ GCT. In deep networks, each convolutional layer always works together with a normalization layer (e.g., BN (Ioffe & Szegedy, 2015)) and an activation layer (e.g., ReLU (Nair & Hinton, 2010)). For this reason, there are three possible points to deploy GCT layer, which are before the convolutional layer, before the normalization layer, and after the normalization layer. All these methods are effective, but we find to be better to employ GNC before the convolutional layer. In Sec. 4.5, we compare the performance of these three application methods.

In the training process, we propose to use 1 to initialize $\boldsymbol{\alpha}$ and use 0 to initialize all $\boldsymbol{\gamma}$ and $\boldsymbol{\beta}$. By doing this, GCT will be initialized as an identity mapping module, which will make the training process more stable. Besides, to avoid the bad influence of unstable gradient on the GCT gate in initial training steps, we propose to use warmup method (to start training with a small learning rate). In all the experiments on ImageNet (Russakovsky et al., 2015) and CIFAR (Krizhevsky & Hinton, 2009), we start training with a learning rate of 0.01 for 1 epoch. After the warmup, we go back to the original learning rate schedule. Finally, we propose **NOT** to apply weight decay on $\boldsymbol{\beta}$ parameters, which is possible to reduce the performance of GCT.

B Experiments on CIFAR

We conduct more experiments on the CIFAR-10 and CIFAR-100 datasets (Krizhevsky & Hinton, 2009). We follow the same training and testing strategies in He et al. (2016a) to conduct our experiments but with a different learning rate schedule. We use a base learning rate of 0.1 and take cosine decay method (Loshchilov & Hutter, 2016) to adjust the learning rate for 300 epochs, which achieves better baseline performance. Following the above training protocol, we start the training process with a learning rate of 0.01 for 1 epoch.

We report the performance of ResNet-110 (He et al., 2016a) and its GCT counterpart in Table 7. To reduce the variances from different runs, we repeat all experiments for 5 times and report the averaged the results. As with the previous experiments, we observe promising improvements in performance, which shows that GCT can generalize to other image classification datasets.

Table 7: **Improvement in top-1 error (%) on the CIFAR-10 and CIFAR-100 datasets.** The numbers in brackets denote the improvement in performance over the baselines.

Dataset	ResNet-110	**GCT**
CIFAR-10	5.81	**5.26**$_{(0.55)}$
CIFAR-100	26.66	**25.77**$_{(0.89)}$

C More Visualization Results

In ResNet-50 (He et al., 2016a) backbone, We visualize the channel activation before and after the GCT layer in both low-level stage (far away from the network output) and high-level stage (close to the output) in Fig.4 and 5, respectively. The input image is from the validation dataset of ImageNet (Russakovsky et al., 2015). As we can see, for the stages far away from the network output, the proposed GCT layer tends to reduce the variance of input feature, which encourages cooperation among channels and avoids excessive activation values or loss of useful features. On the contrary, for those stages close to the output, GCT tends to magnify the variance. Here, GCT acts like the attention mechanism that is useful for creating competition.

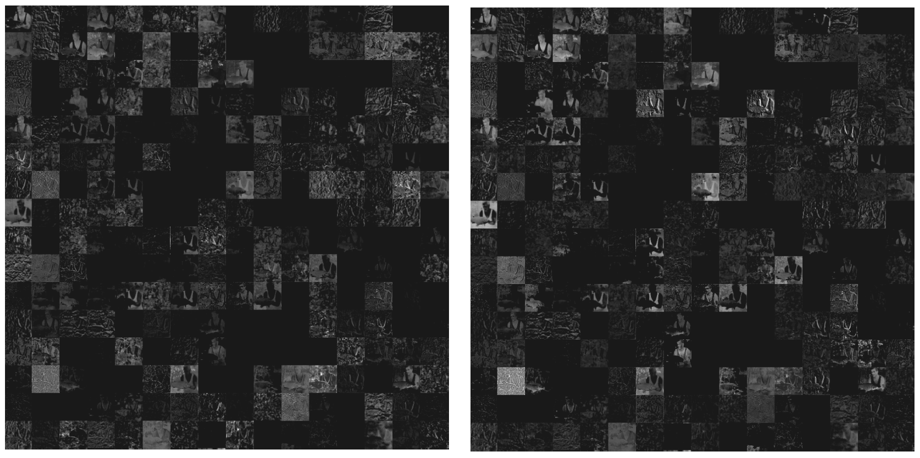

(a) Before GCN (b) After GCN

Figure 4: Visualization of the channel activation for a GCT layer in Stage 2 (low-level) of ResNet-50 on the validation dataset of ImageNet.

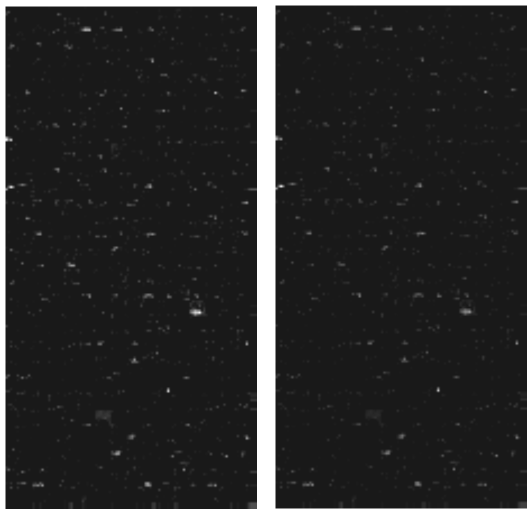

(a) Before GCN (b) After GCN

Figure 5: Visualization of the channel activation for a GCT layer in Stage 5 (high-level) of ResNet-50 on the validation dataset of ImageNet.